Ab Initio Studies of Nonlinear Optical Properties of 2D Semiconductors

Guang-Yu Guo (郭光宇)

Physics Dept, National Taiwan University, Taiwan

（國立臺灣大學物理系）

(Talk in NCTS Workshop on TDDFT and Excited State Properties of Solids, NTU, May 17-18, 2016)

Acknowledgements

Collaborators:

Chung-Yu Wang, Ren-Bo Wang, Cheng-You Liu
(Physics Dept., NTU)

Financial Supports:

Ministry of Science and Technology of Taiwan
Thematic Research Program of Academia Sinica

[*arXiv:1409.0937v2; J. Phys. Chem. C 119, 13268 (2015)]

Outline

I. Introduction

1. Novel properties induced by transition from bulk to monolayers
2. Motivations

II. Theory and computational method

1. Linear response theory of the optical properties
2. *Ab initio* calculations using the VASP and home-made utility codes

III. Second-harmonic generation of MX_2 monolayer and trilayers

1. Electronic structure and optical properties of monolayers
2. Electronic structure and optical properties of trilayers
3. Comparison with experiments and previous calculations

IV. Second-harmonic generation of III-VI bulks and monolayers

1. Electronic structures of crystals and monolayers
2. Nonlinear optical properties of crystals and monolayers

V. Future work

Excitonic effect and time-propagation approach

I. Introduction

1. Novel properties induced by transition from bulk to monolayers

1) Layered transition metal dichalcogenides [Wilson, Yoffe, Adv. Phys. 18 (1969) 193]

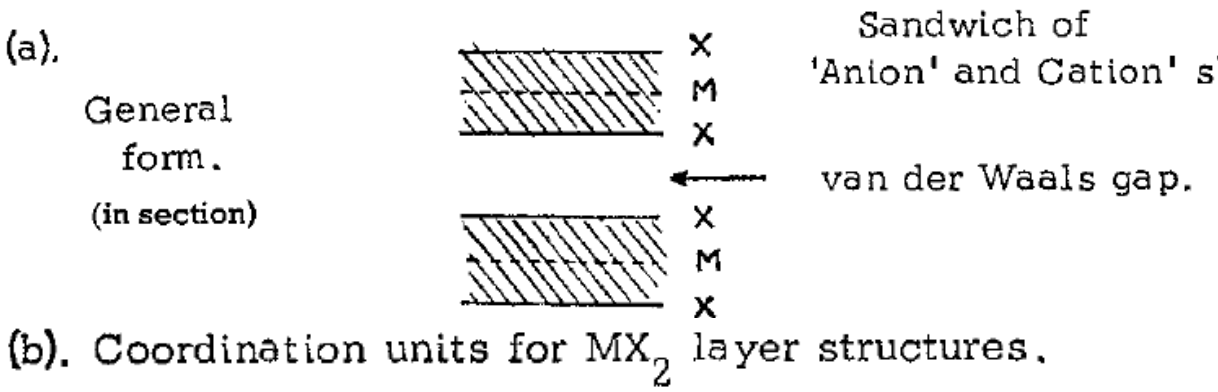

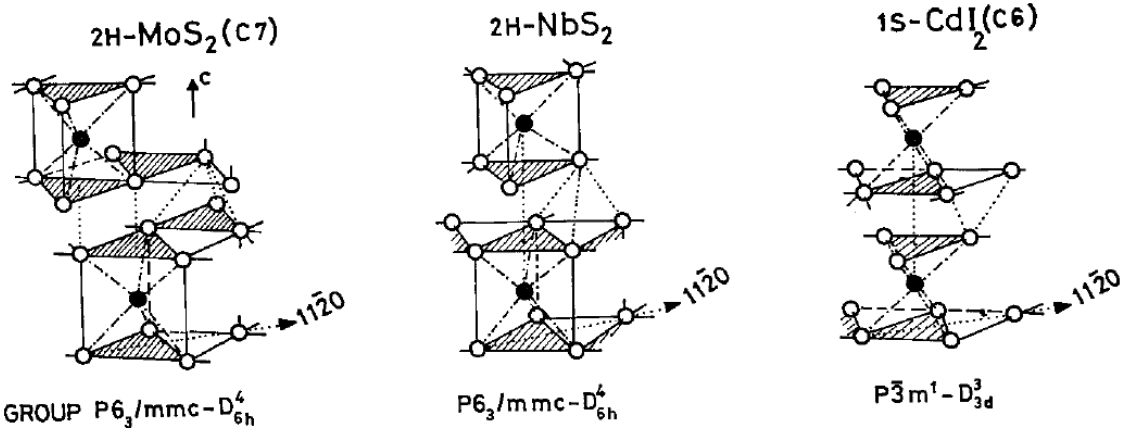

Physically, the compounds have widely different electrical and optical properties, e.g., CDW and superconductivity phase transition.

Chemically, they may be intercalated by Lewis bases, resulting in pronounced property changes.

Mechanically, they could be easily cleaved to prepare thin films.

2) Transformation from bulk to monolayers

3D bulk crystals

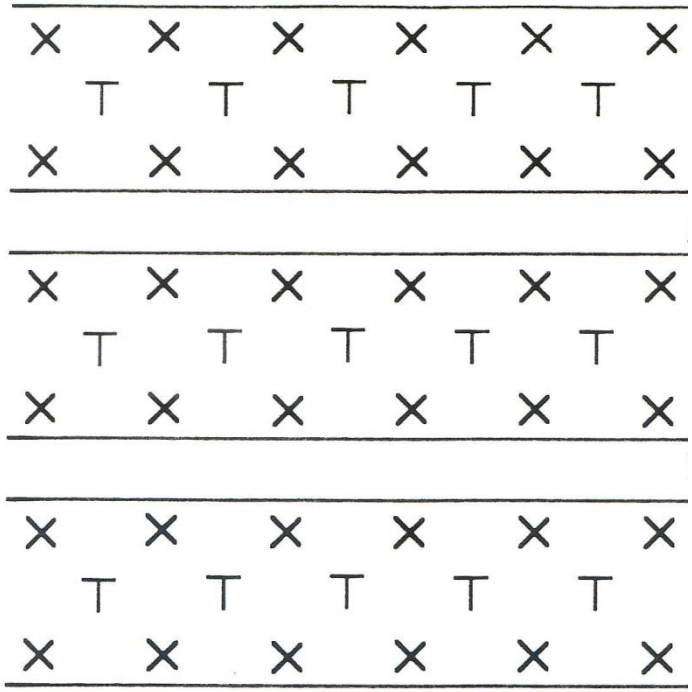

40 years

by exfoliation etc.

2D monolayers

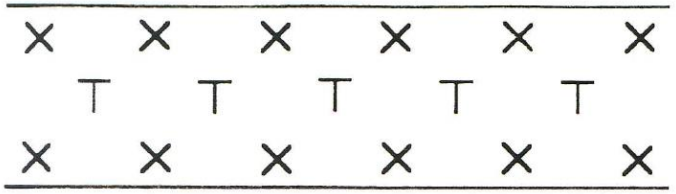

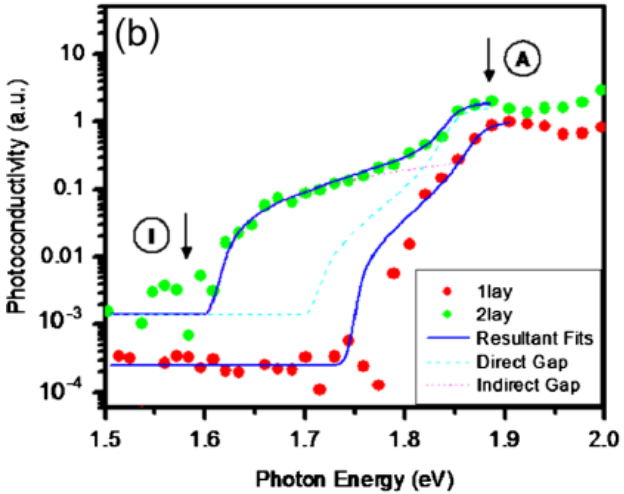

[Mak et al., PRL 105 (2010) 136805]

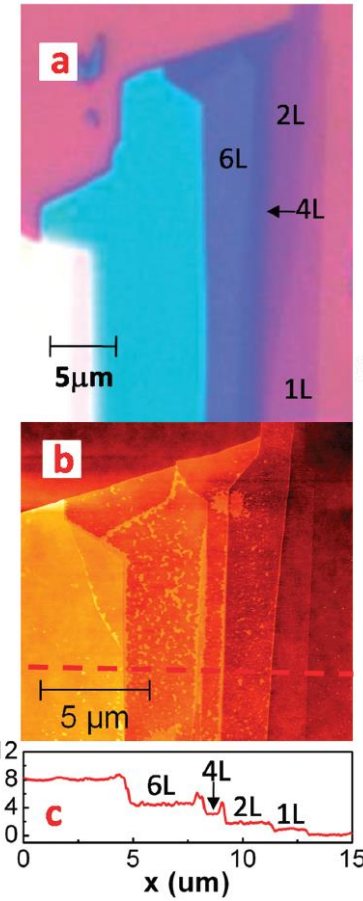

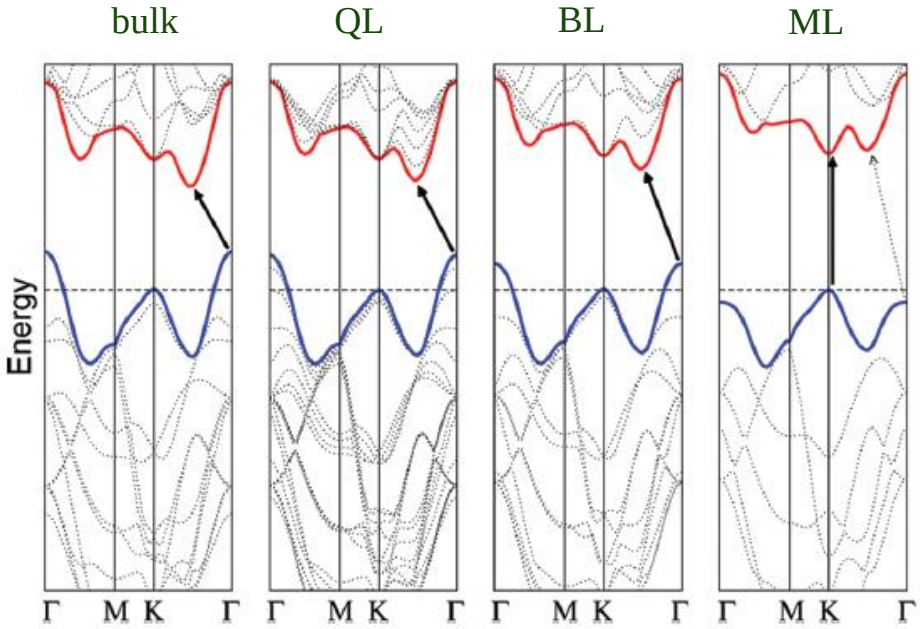

[Splendiani et al., NL 10 (2010) 1271]

Two major structural changes

(1) Truly 2D layered systems

Physical effects:

(a) from indirect to direct band gap

[PRL 105 (2010) 136805; PRB 87 (2013) 155304],

(b) 2D superconductivity, CDW

etc.

(2) Broken inversion symmetry

Physical effects:

(a) SOC band splittings [PRB 84 (2011) 153402]:

spintronics and valleytronics [PRL 108 (2012) 196802]

(b) Piezoelectrics [J.Phys.Chem.Let. 3 (2012) 2871]

(c) Second-order nonlinear optical property

[PRB 87 (2013) 161403; 87 (2013) 201401; NL 13 (2013) 3329]

etc

2. Motivations

(1) Second-harmonic generation in odd-number layers of MX_2

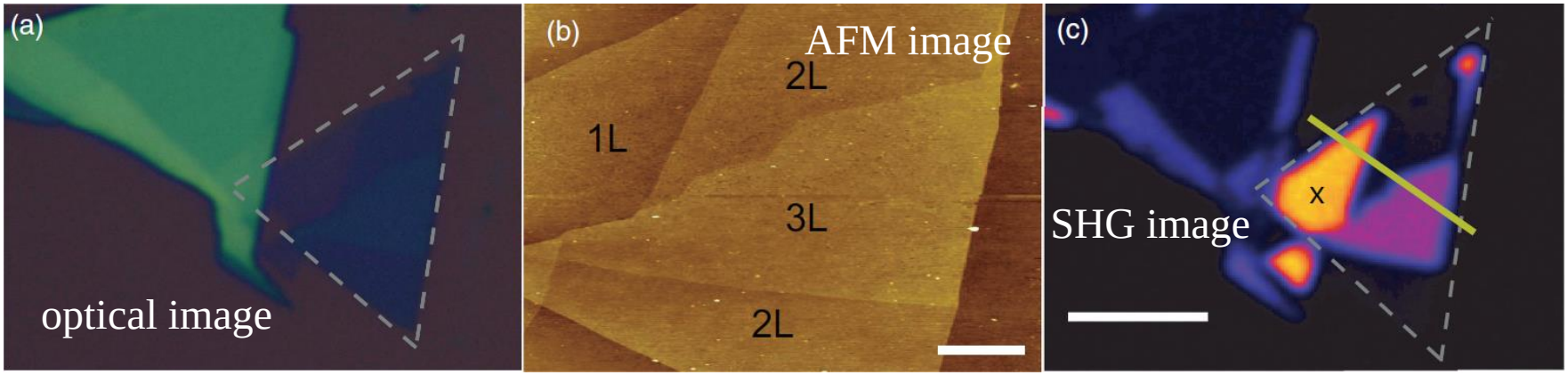

MX_2 (M = Mo, W; X = S, Se) monolayers possess significant second-order nonlinear optical susceptibility.

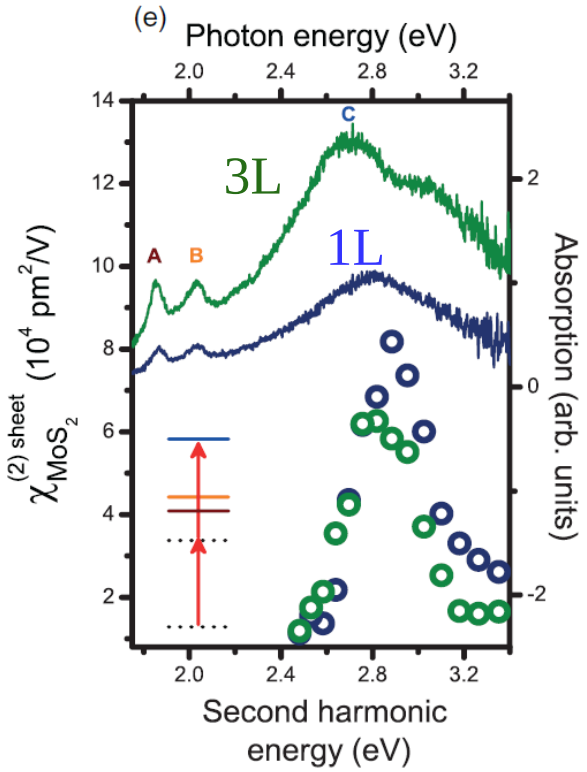

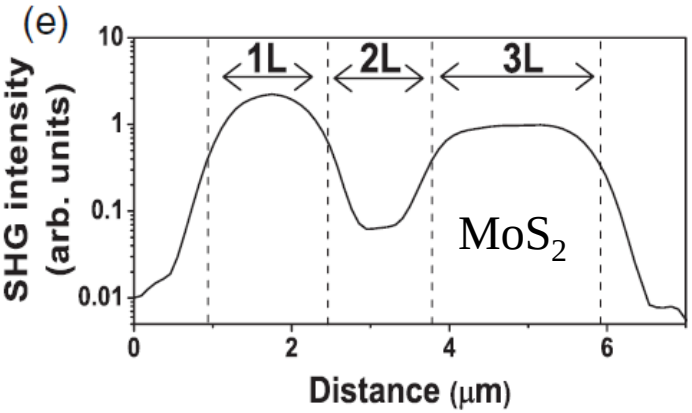

[Malard et al., PRB 87 (2013) 201401(R)]

(2) Applications of few layers of MX_2

[Malard et al., PRB 87 (2013) 201401(R)]

They are promising materials for non-linear optical devices and electro-optical applications.

The non-linear optical property (second harmonic generation) can also be exploited to characterize the crystalline structure and orientation of the few monolayers MX_2 materials. (GaAs: $|\chi^{(2)}(0)|$ = ~200 pm/V)

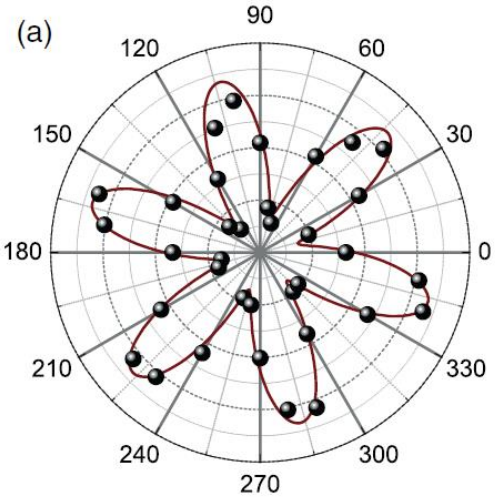

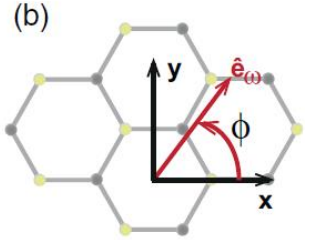

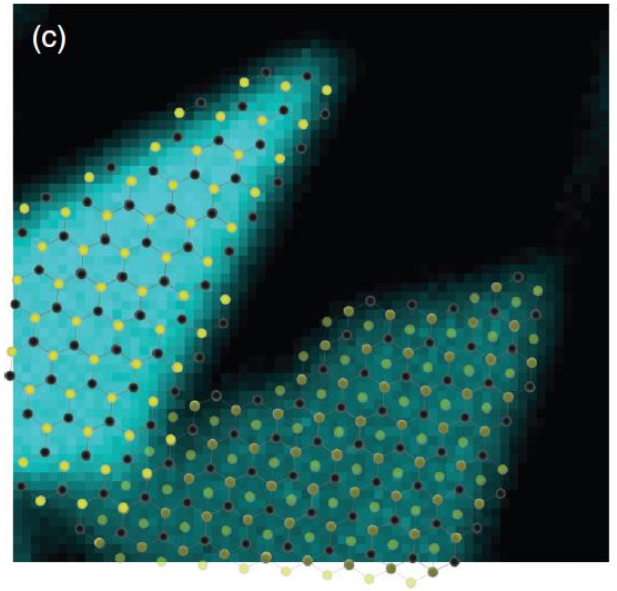

Under 810 nm (1.53 eV) wavelength, measured $|\chi^{(2)}|$

$|\chi^{(2)}|$ = 322 pm/V; Li et al., NL 13 (2013) 3329.

$|\chi^{(2)}|$ = 82 pm/V; PRB 87 (2013) 201401.

$|\chi^{(2)}|$ = 10^5 pmV; Kumar et al., PRB 87 (2013).

(3) A systematic ab initio study of SHG of all MX_2 (M = Mo, W; X = S, Se) monolayers and trilayers is thus carried out in this work.

(4) MX (M = Ga, In; X = S, Se) semiconductor bulks and monolayers

bulk structural polytypes

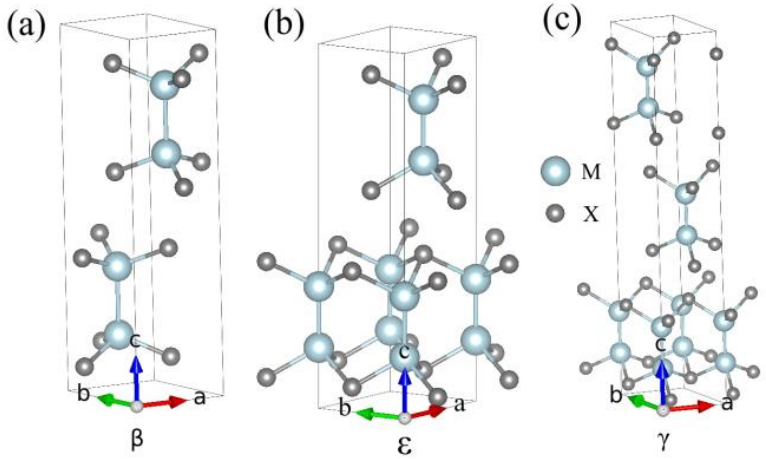

monolayer structure

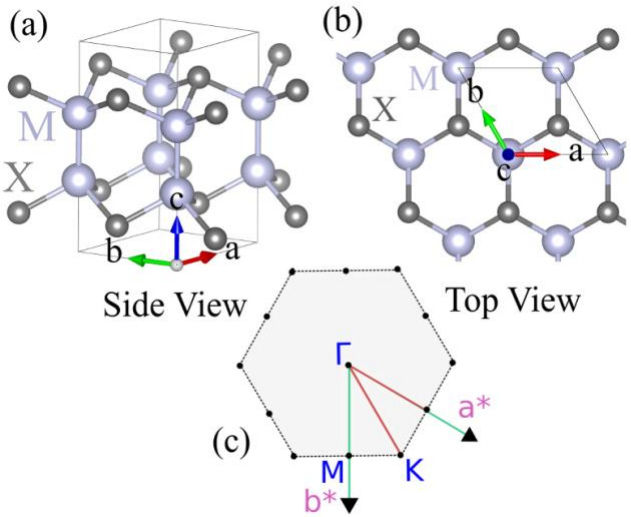

Layered semiconductors having
electronic and optoelectronic applications
nonlinear optical properties (ε, γ polytyes)

Monolayer flakes of MX are obtained by exfoliation or grown on substrates by CVD.

Optical band gap increases,
e.g., 1.8 (direct) → 3.2 eV (indirect) (GaSe)
High mobility > 10^3 cm^2/Vs (InSe) for FET.

tunable magnetism in p-type GaSe ML

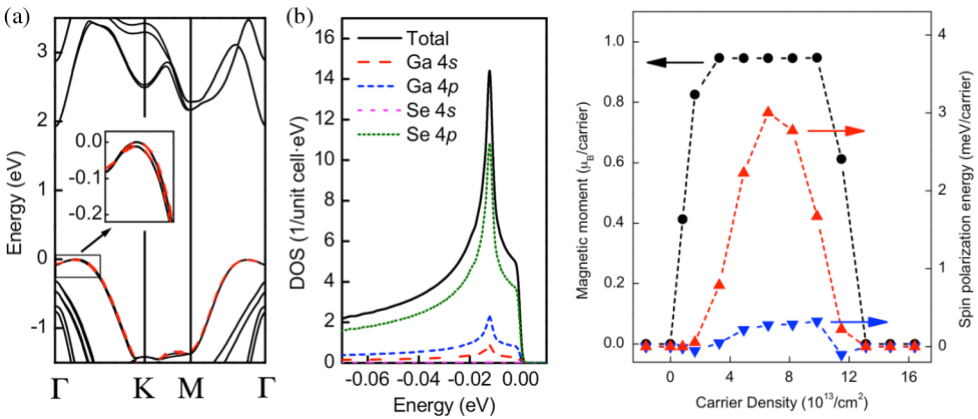

[Cao et al., PRL114 (2015) 236602]

Strong SHG in GaSe MLs

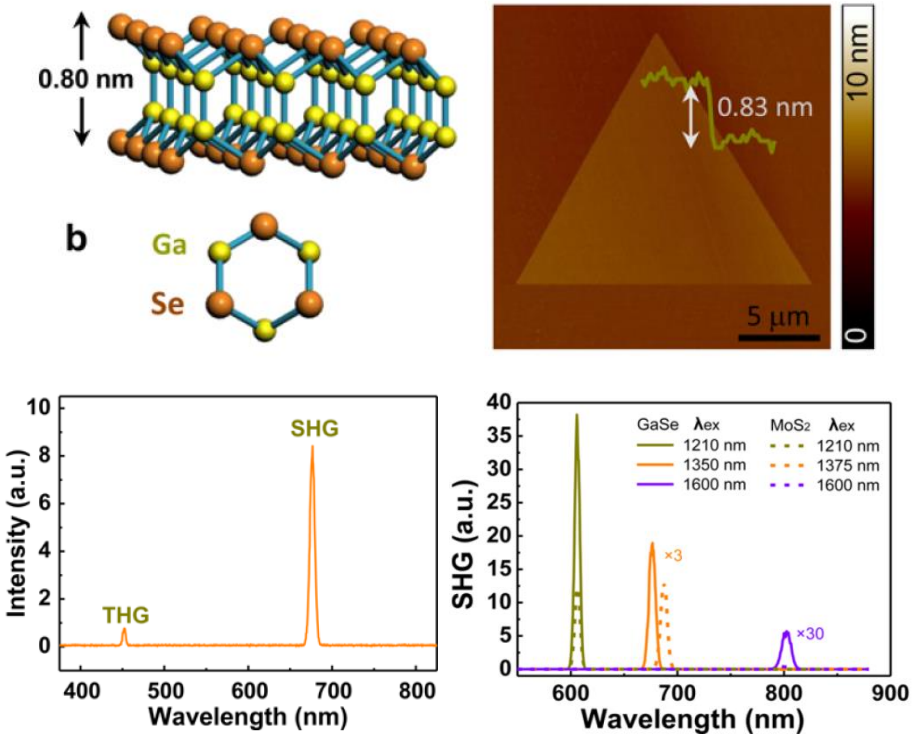

[Zhou et al., JACS 137 (2015) 7994]

Under 1.60 μm (0.77 eV)
$|\chi^{(2)}|$ = 700 pm/V (GaSe);
$|\chi^{(2)}|$ = 430 pm/V (MoS2)

Under 1.21 μm (1.02 eV)
$|\chi^{(2)}|$ = 2400 pm/V (GaSe).

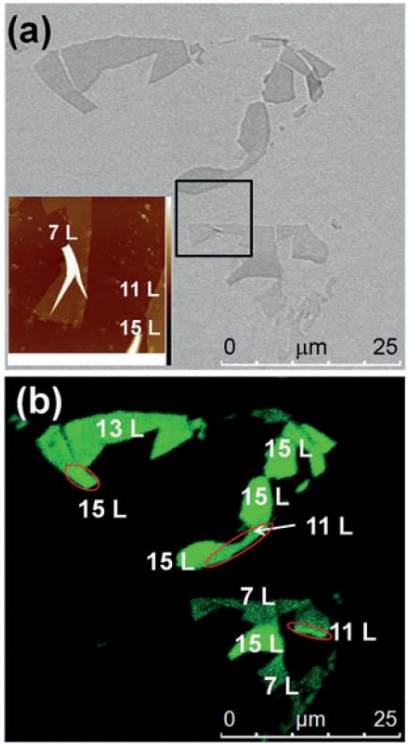

Confocl laser microscope of GaSe flakes on glass

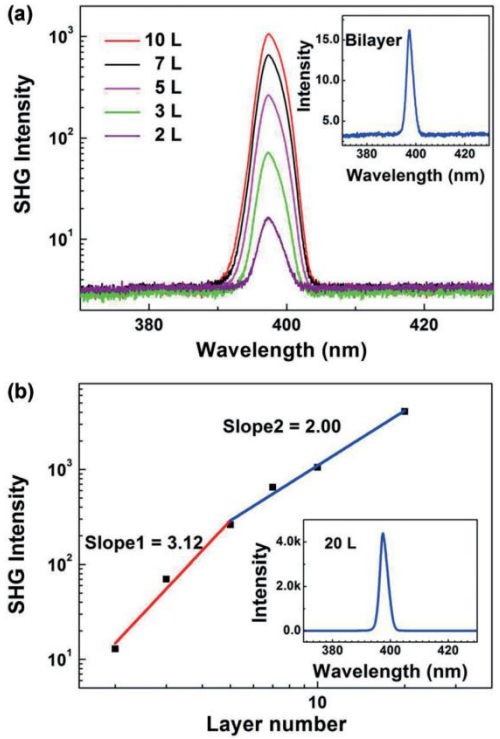

SHG of GaSe thin films

[Jie et al., Angew. Chem. Int. Ed. 54 (2015) 1185]

Under 978 nm (1.268 eV) $|\chi^{(2)}|$
$|\chi^{(2)}|$ = 60 pm/V (BL)
$|\chi^{(2)}|$ = 93 pm/V (TL).

II. Theory and computational method

1. Linear response theory of the optical properties

The optical properties are calculated within the independent particle approximation (IPA) from the Kohn-Sham eigenstates, i.e., the excitonic effects and the local-field effects are neglected.

Dielectric functions

(Fermi golden rule)

$$\varepsilon'' = \frac{4\pi^2}{\Omega\omega^2} \sum_{\mathbf{k},n,n'} |\left\langle \mathbf{k}n' \middle| \hat{p}_i \middle| \mathbf{k}n \right\rangle|^2 \times \delta(\varepsilon_{\mathbf{k}n'} - \varepsilon_{\mathbf{k}n} - \hbar\omega).$$

(Kramer-Kronig transformation)

$$\varepsilon'(\omega') = 1 + \frac{2}{\pi^2} \mathbf{P} \int_0^\infty d\omega' \frac{\omega' \varepsilon''(\omega')}{(\omega'^2 - \omega^2)}.$$

Second-order optical susceptibility

$$\chi''^{(2)}_{abc}(-2\omega,\omega,\omega) = \chi''^{(2)}_{abc,VE}(-2\omega,\omega,\omega) + \chi''^{(2)}_{abc,VH}(-2\omega,\omega,\omega),$$

$$\chi''^{(2)}_{abc,VE} = -\frac{\pi}{2}\sum_{i\in VB}\sum_{j,l\in CB}\sum_{\mathbf{k}} w_{\mathbf{k}}\{\frac{\mathrm{Im}[\,p^a_{jl}\{p^b_{li}p^c_{ij}\}]}{E^3_{li}(E_{li}+E_{ji})}\delta(E_{li}-\omega) - \frac{\mathrm{Im}[\,p^a_{ij}\{p^b_{jl}p^c_{li}\}]}{E^3_{li}(E_{li}-E_{ji})}\delta(E_{li}-\omega)$$
$$+\frac{16\mathrm{Im}[\,p^a_{ij}\{p^b_{jl}p^c_{li}\}]}{E^3_{ji}(E_{li}-E_{ji})}\delta(E_{ji}-2\omega)\},$$

$$\chi''^{(2)}_{abc,VH} = \frac{\pi}{2}\sum_{i,l\in VB}\sum_{j\in CB}\sum_{\mathbf{k}} w_{\mathbf{k}}\{\frac{\mathrm{Im}[\,p^a_{li}\{p^b_{ij}p^c_{jl}\}]}{E^3_{jl}(E_{jl}+E_{ji})}\delta(E_{jl}-\omega) - \frac{\mathrm{Im}[\,p^a_{ij}\{p^b_{jl}p^c_{li}\}]}{E^3_{jl}(E_{jl}-E_{ji})}\delta(E_{jl}-\omega)$$
$$+\frac{16\mathrm{Im}[\,p^a_{ij}\{p^b_{jl}p^c_{li}\}]}{E^3_{ji}(E_{jl}-E_{ji})}\delta(E_{ji}-2\omega)\},$$

$$E_{ji} = E_j(\mathbf{k}) - E_i(\mathbf{k}),\ p_{ij} =< j\mathbf{k} \mid \hat{p} \mid i\mathbf{k} >, \{p^b_{jl}p^c_{li}\} = \tfrac{1}{2}\{p^b_{jl}p^c_{li} + p^b_{jl}p^c_{li}\}.$$

$$\chi'^{(2)}(-2\omega',\omega,\omega) = \frac{2}{\pi}\mathbf{P}\int_0^\infty d\omega'\frac{\omega'}{(\omega'^2-\omega^2)}\chi''^{(2)}(-2\omega',\omega,\omega).$$

2. Ab initio calculations using the VASP and home-made utility code

(1) Electronic band structure calculations using the VASP code:

Density-functional theory (DFT)-Generalized gradient approximation (GGA);

Projector augmented-wave (PAW) method;

Slab-supercell approach with interlayer separation $d > 18$ Å ;

BZ integration: 20×20×1 $\boldsymbol{k}$-mesh;

Plane-wave energy cutoff $E_{\text{cut}} = 400$ eV;

(2) Optical property calculations using the home-made utility code:

In IPA, the optical properties are calculated using the dipole transition matrix elements and Kohn-Sham eigenvalues generated by the VASP code;

BZ integration: a denser 130×130×1 [100×10×1] ***k***-mesh is used for monolayers [trilayers];

More than 25 energy bands per atom are included in the calculations.

Excitonic effects on linear optical properties of 2D materials are strong. Nonetheless, in some cases, they appear to be washed out to some extent. Thus, the IPA+scissors correction approach seems to be capable of producing reasonable results in some cases. On the other hand, this simpler approach allows one to use a sufficiently dense k-mesh and to include sufficiently large number of empty bands, which are crucial to get numerically converged SHG.

III. Second-harmonic generation of MX_2 monolayers and trilayers

1. Second-order nonlinear optical susceptibility of monolayers

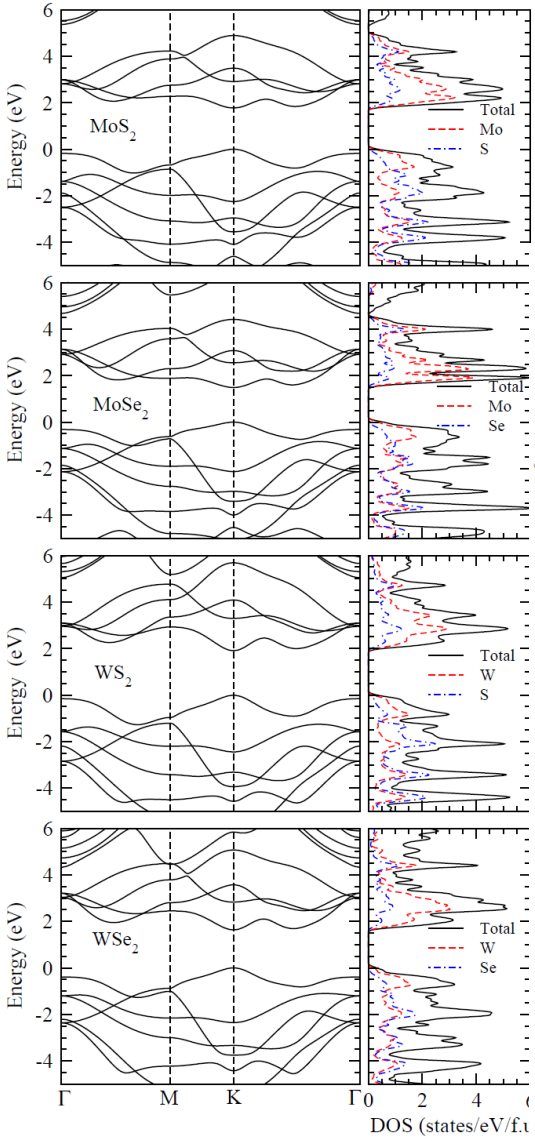

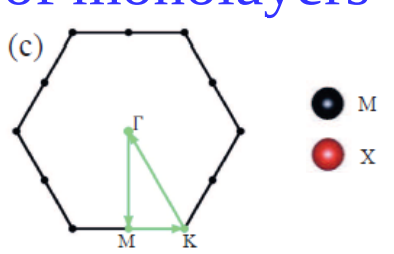

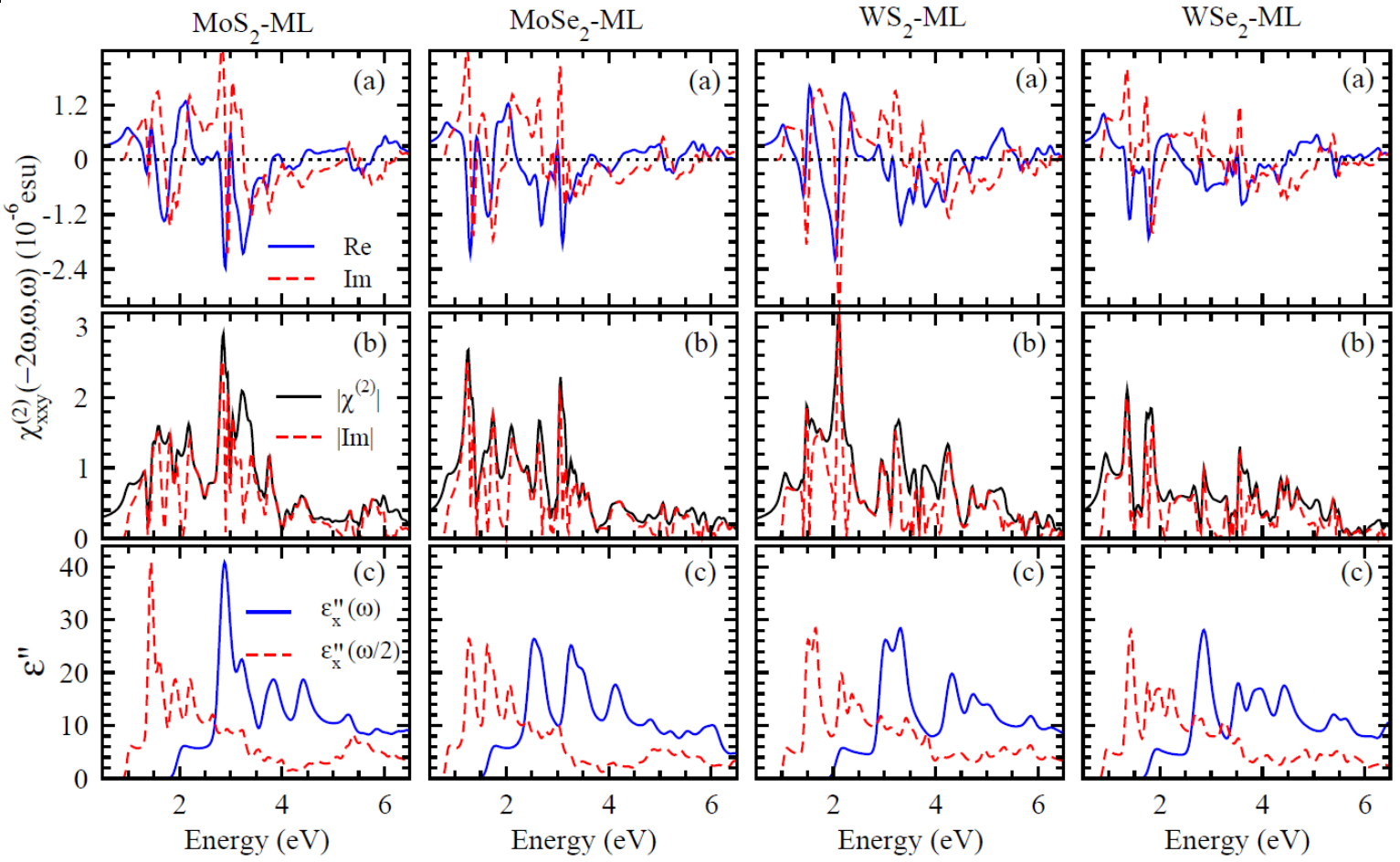

2. Second-order nonlinear optical susceptibility of trilayers

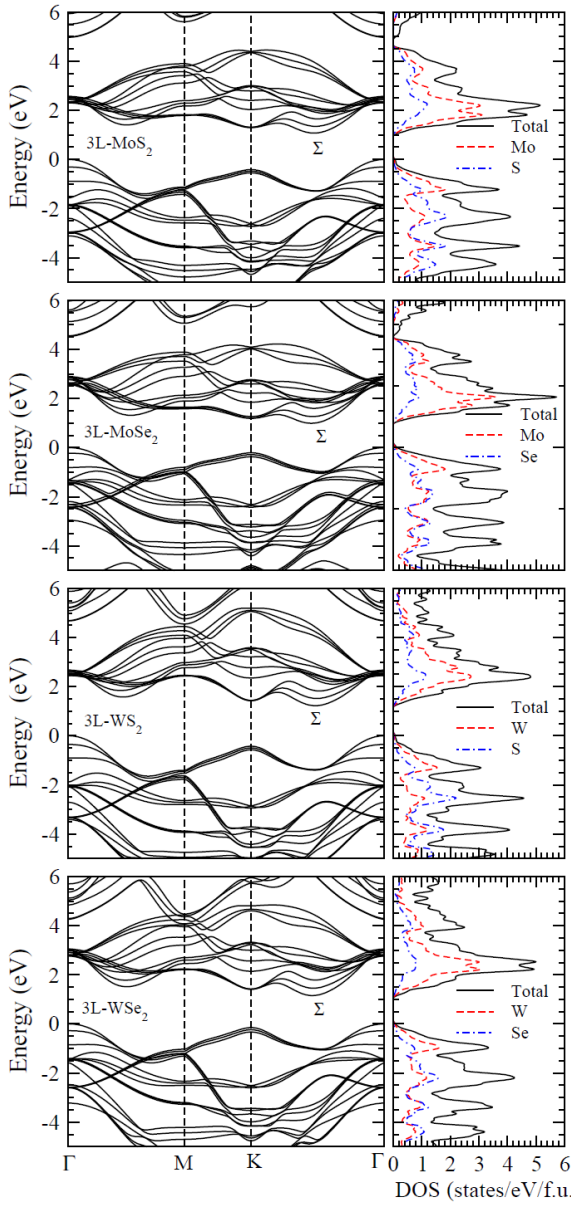

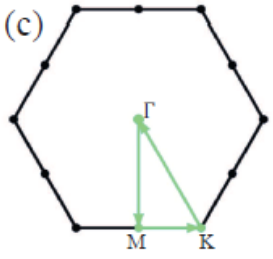

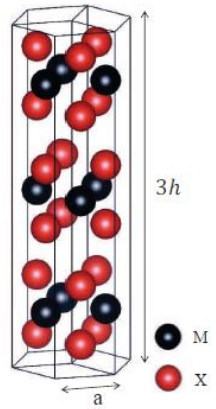

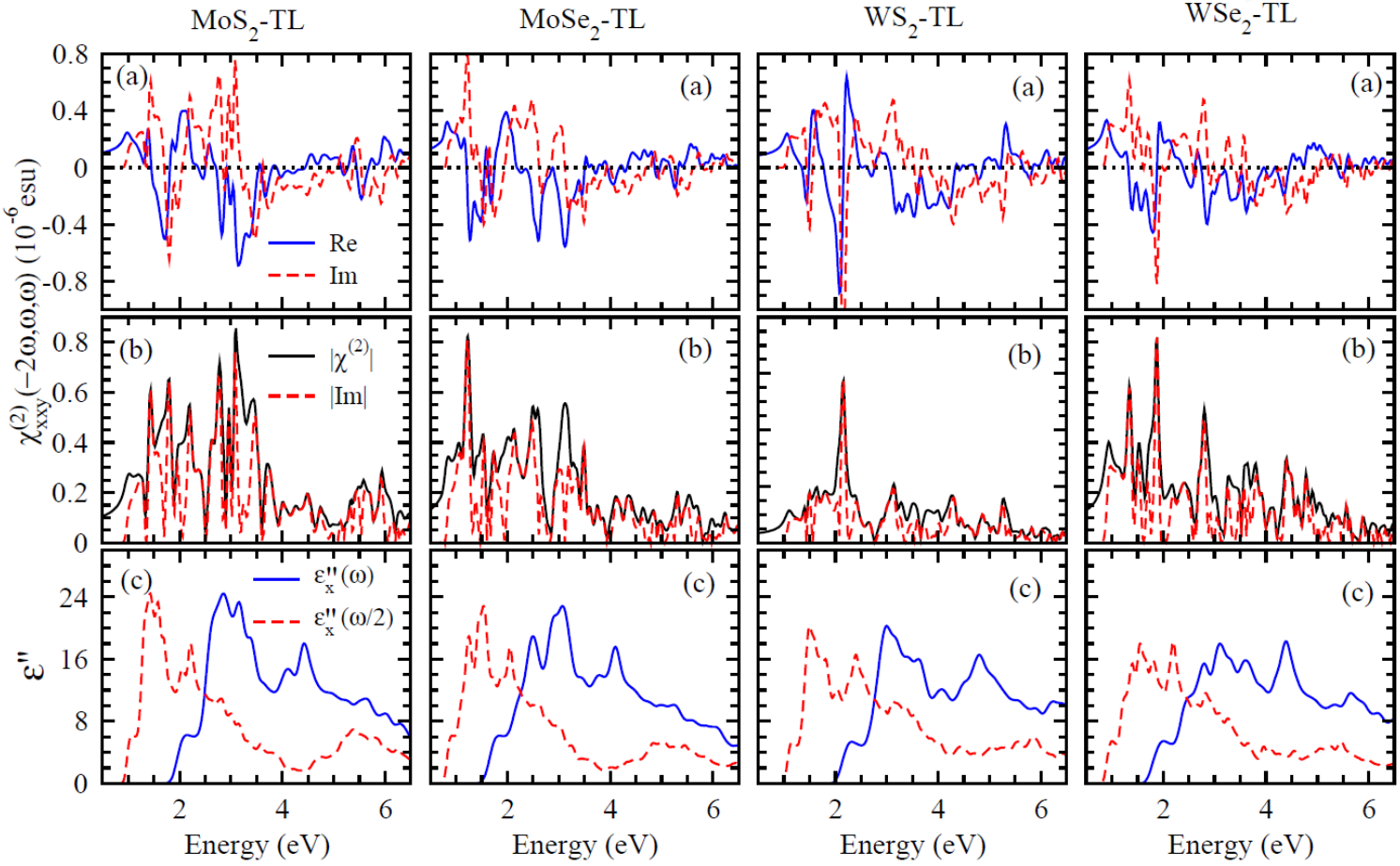

[arXiv: 1409.0937v2]

TABLE III. Calculated static refraction index (n_x), second-order optical susceptibility $\chi^{(2)}(0)$, $|\chi^{(2)}(1.53\ \text{eV})|$ and linear electro-optical coefficient r_{xxy} of the MX_2 MLs (a) and TLs (b) using the band structures without (IPA) and with (SCI) scissors correction. The available experimental values (exp.) are also listed.

		MoS_2	$MoSe_2$	WS_2	WSe_2
(a) MLs					
n_x	IPA	3.92	3.91	3.76	3.75
	SCI	3.65	3.64	3.48	3.51
$\chi^{(2)}_{xxy}(0)$ (pm/V)	IPA	141	170	125	177
	SCI	109	128	93	132
$\lvert\chi^{(2)}_{xxy}(1.53)\rvert$ (pm/V)	IPA	847	558	819	227
	SCI	573	449	712	163
	exp.	322[a],82[b]			
	exp.[c]	10^5,5000			
$r_{xxy}(0)$(pm/V)	IPA	-1.19	-1.45	-1.25	-1.79
	SCI	-1.23	-1.46	-1.26	-1.74
(b) TLs					
n_x	IPA	3.96	3.93	3.79	3.78
	SCI	3.69	3.55	3.51	3.54
$\chi^{(2)}_{xxy}(0)$ (pm/V)	IPA	49	58	43	58
	SCI	38	44	31	44
$\lvert\chi^{(2)}_{xxy}(1.53)\rvert$ (pm/V)	IPA	257	158	257	144
	SCI	164	180	267	166
	exp.	80[a],17[b]			
$r_{xxy}(0)$(pm/V)	IPA	0.39	0.43	0.40	0.35
	SCI	0.40	0.43	0.40	0.35
(c) TLs vs. MLs					
$\chi^{(2)}_{TL}(0)/\chi^{(2)}_{ML}(0)$	IPA	0.35	0.34	0.34	0.33
	SCI	0.35	0.34	0.34	0.33
$\chi^{(2)}_{TL}/\chi^{(2)}_{ML}(1.53)$	IPA	0.30	0.28	0.31	0.63
	SCI	0.28	0.40	0.39	1.02
	exp.	0.25[a],0.21[b]		0.60[d]	0.93[d]

[17] Malard et al., PRB 89 (2013) 201401.
[18] Gruning, Attaccalite, PRB 89 (2014) 081102.
[19] Trolle et al., PRB 89 (2014) 235410.

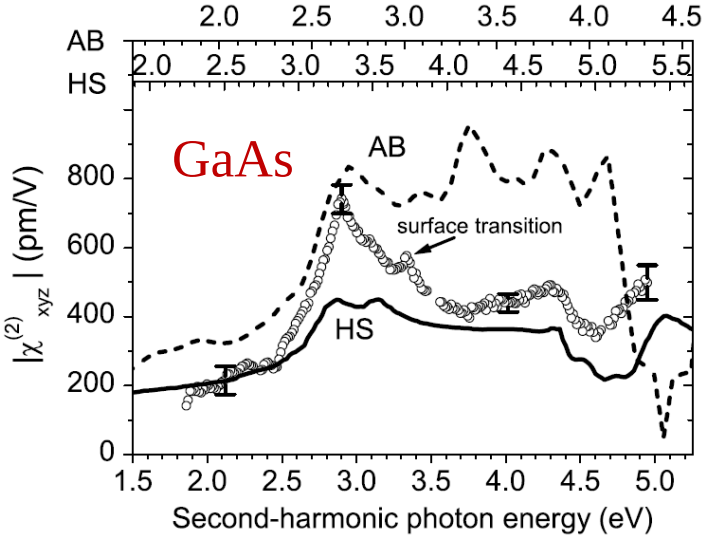

[Bergfeld & Daum, PRL 90 (2003) 036801]

If there is no interlayer coupling,
$|\chi^{(2)}_{TL}|/|\chi^{(2)}_{ML}| \sim 1/3$.
Linear electro-optical coefficients r_{xxy} in low-frequency limit are significant.

3. Comparison with experiments and previous calculations

All IPA results agree with each other.

Experimental spectrum [17] agrees with IPA spectra in shape but small in magnitude.

Real-time calculations roughly agrees with present scissors corrected results.

TB calculations have a magnitude being 5 times larger, and blue-shifted energy positions of the major features.

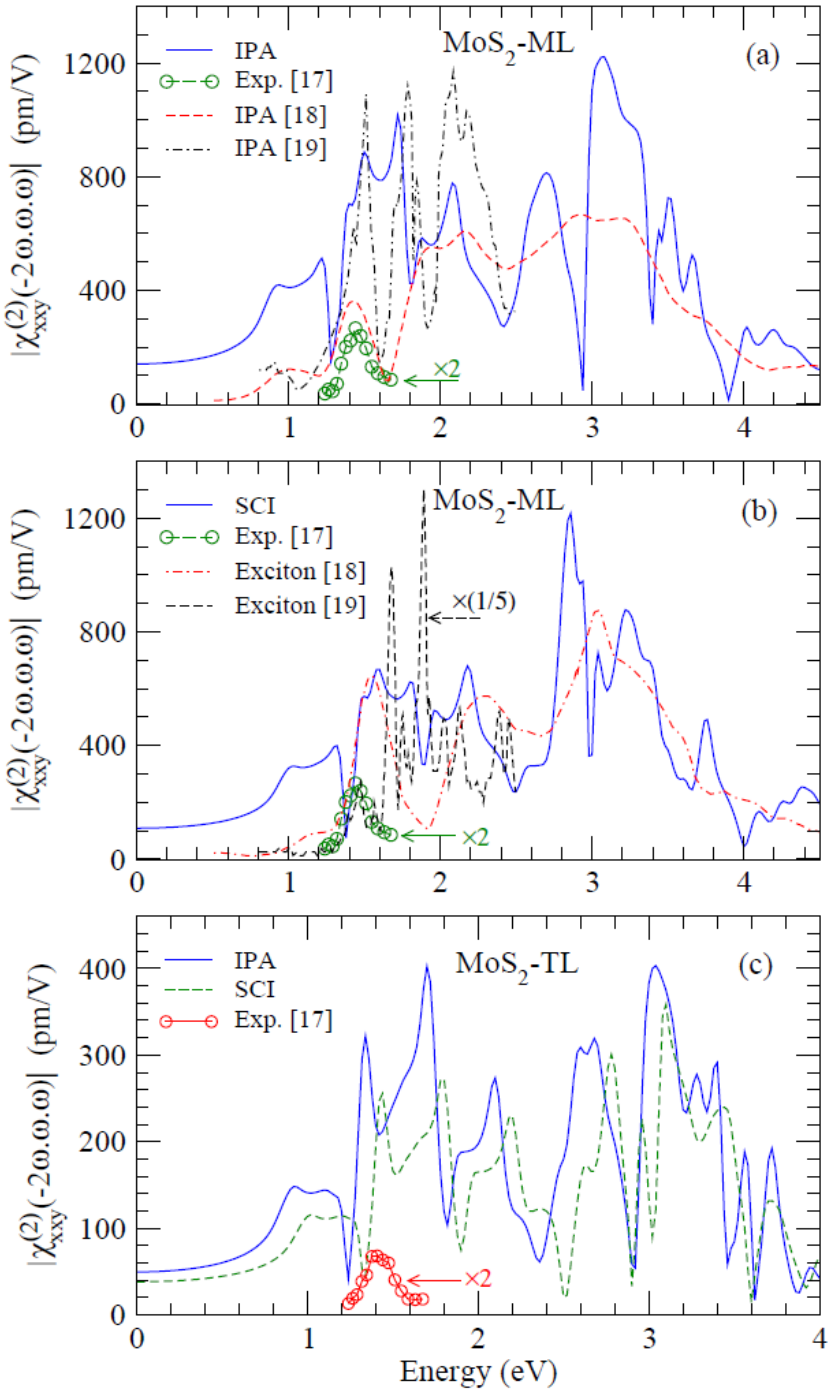

[17] Malard et al., PRB 89 (2013) 201401.
[18] Gruning, Attaccalite, PRB 89 (2014) 081102.
[19] Trolle et al., PRB 89 (2014) 235410.

IV. Second-harmonic generation of III-VI bulks and monolayers

1. Electronic structures of crystals and monolayers

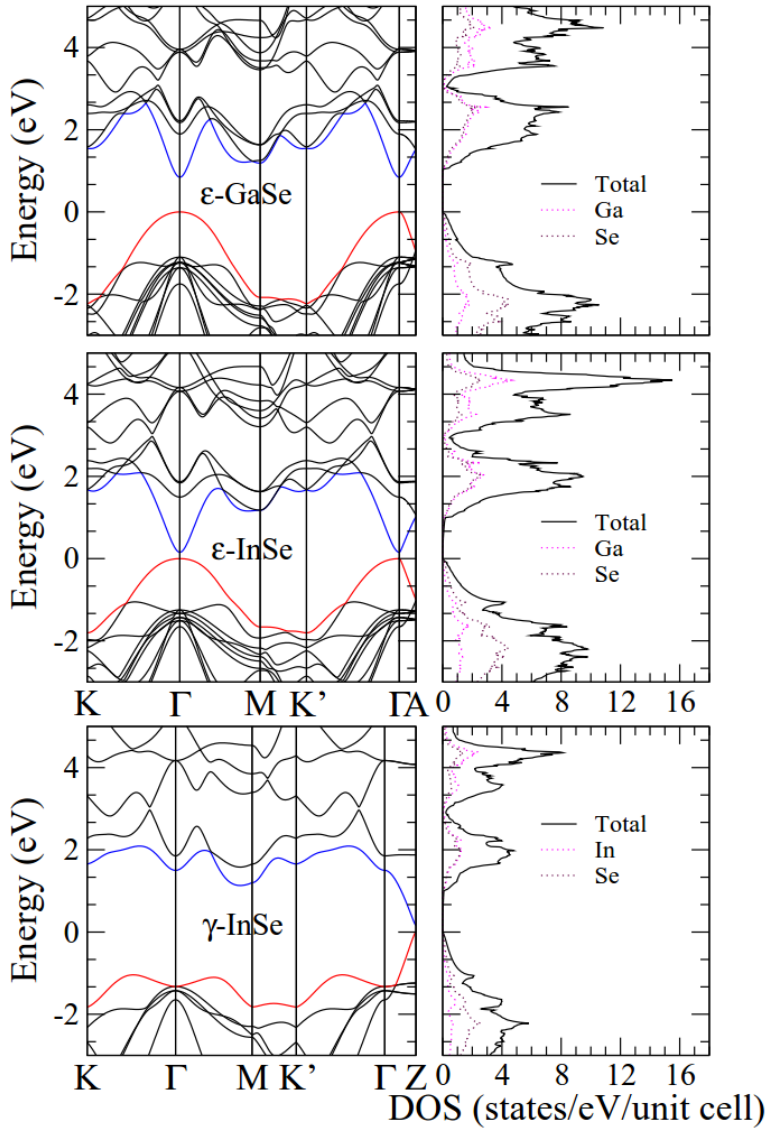

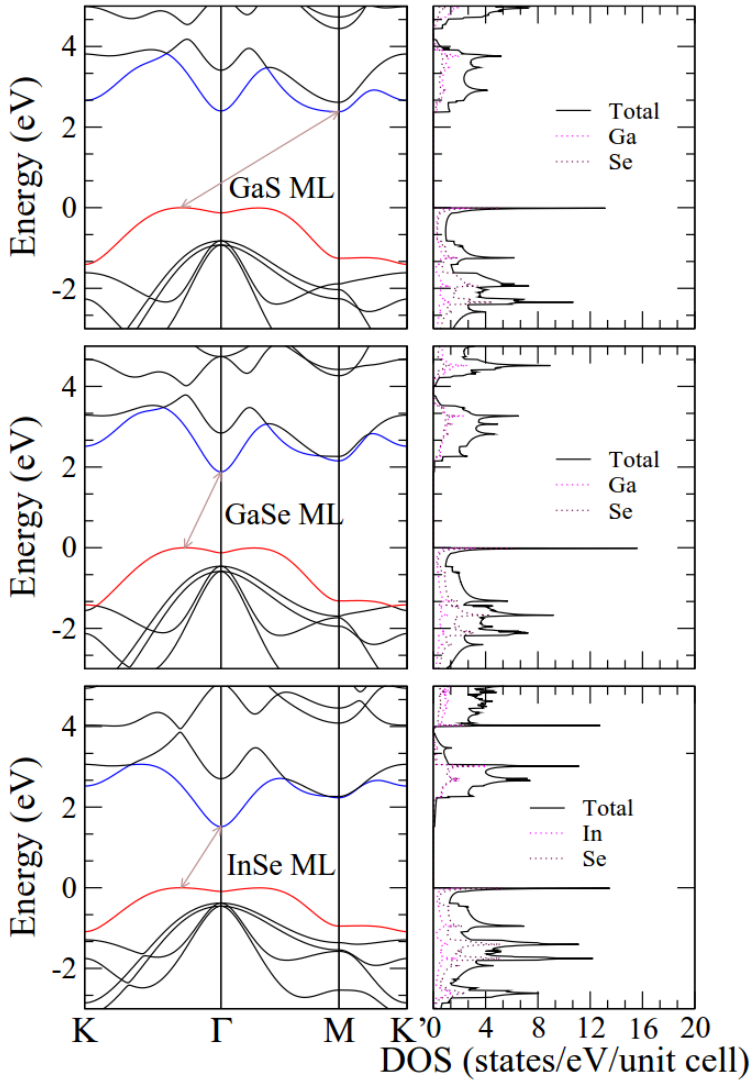

2. Nonlinear optical properties of crystals and monolayers

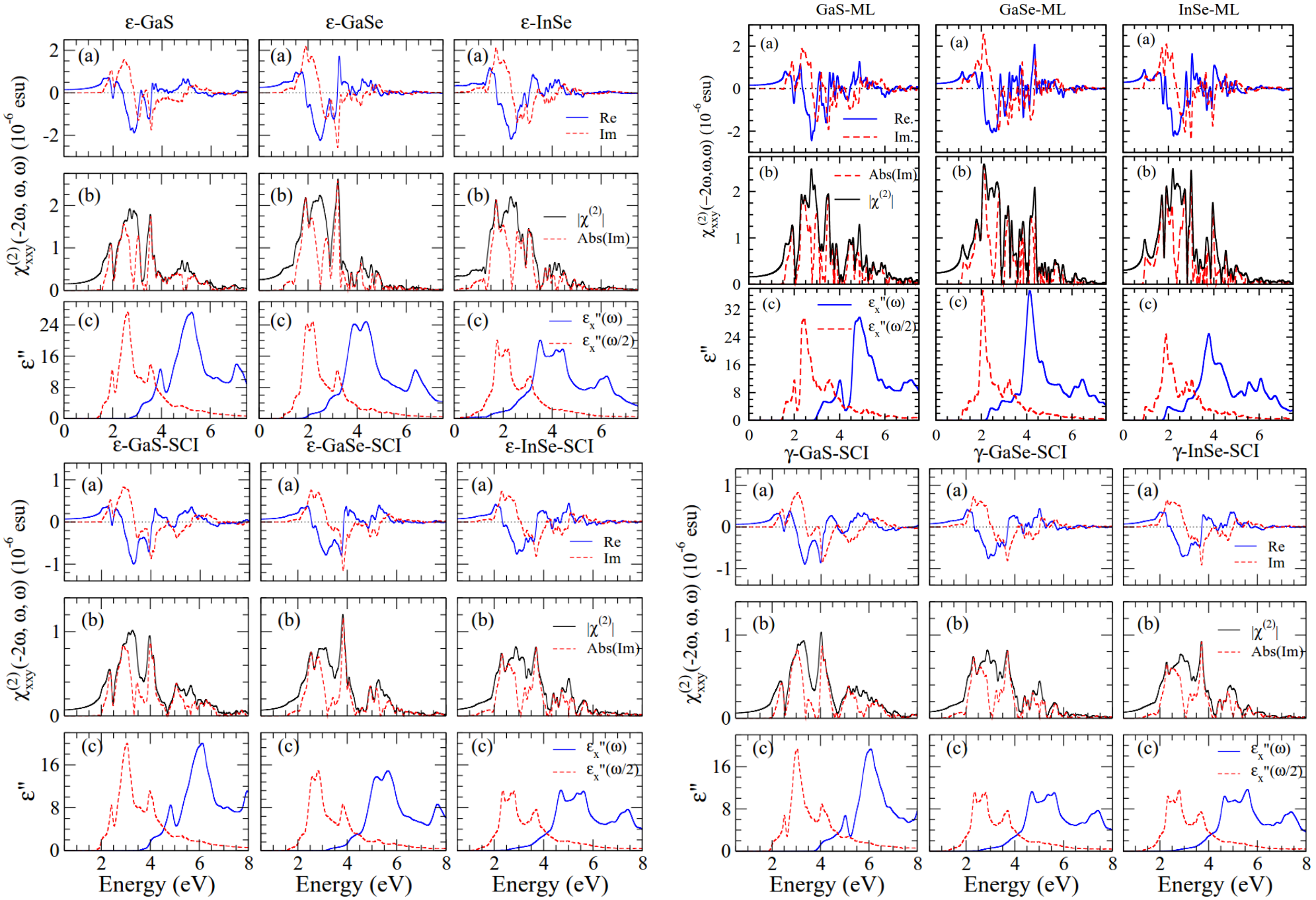

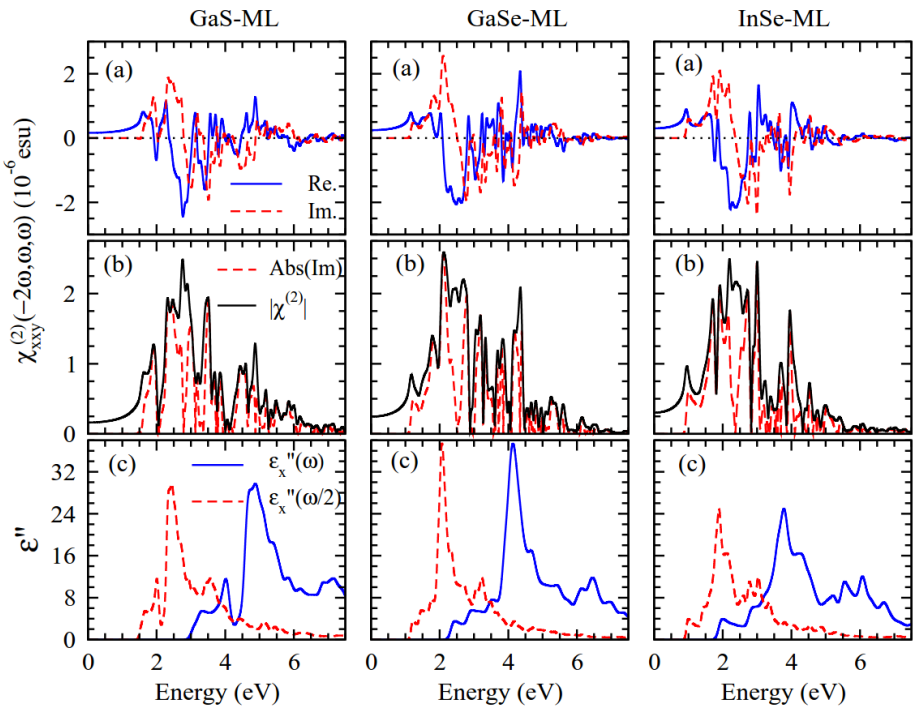

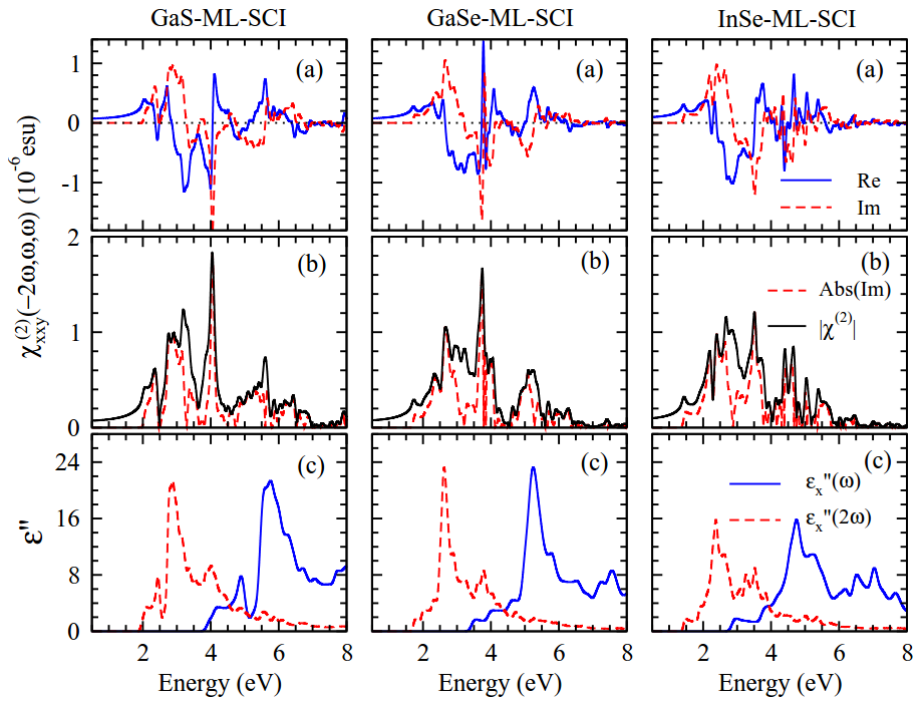

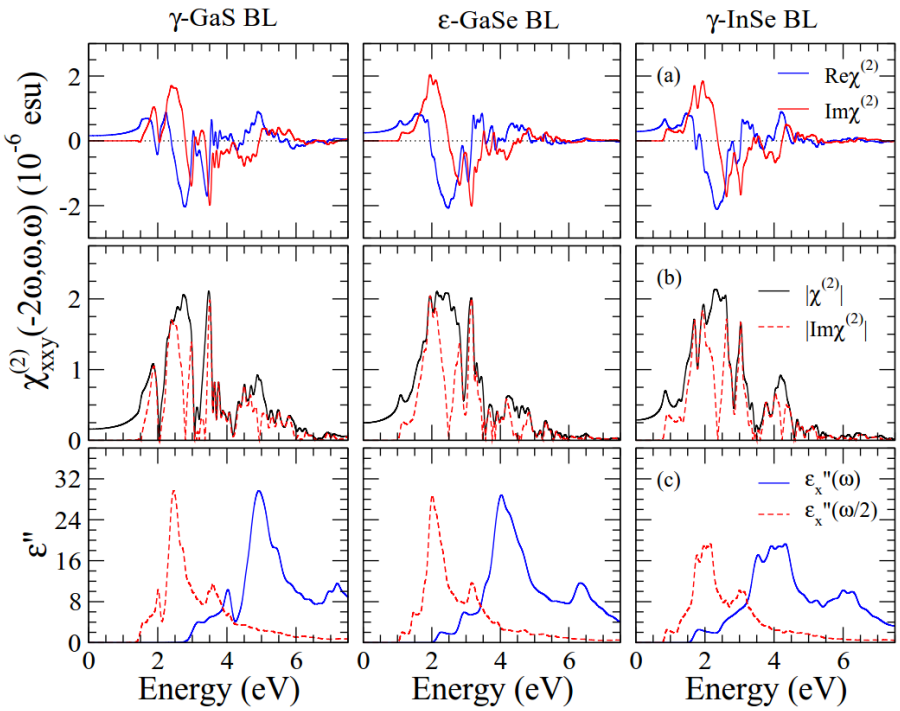

		GaS ML (BL)	GaSe ML (BL)	InSe ML (BL)
E_g (eV)	LDA	2.38 (1.94)	1.88 (1.52)	1.44 (0.98)
	HSE	3.27 (2.82)	2.99 (2.54)	2.49 (1.91)
	Exp	3.05[a]	3.3[b]	1.54[c]
$n_x(0)$	LDA	2.96	3.07	3.03
	SCI	2.45	2.34	2.33
$\chi^{(2)}_{xxy}(0)$ (pm/V)	LDA	68 (67)	103 (104)	126 (121)
	SCI	29	30	38
$\chi^{(2)}_{xxy}(0.77)$ (pm/V)	LDA	84 (82)	142 (144)	213 (231)
	SCI	33	36	49
	Exp		700	
$\chi^{(2)}_{xxy}(1.27)$ (pm/V)	LDA	133 (130)	278 (233)	241 (240)
	SCI	43	50	79
	Exp		(60)	
$r_{xxy}(0)$ (pm/V)	LDA	1.77	2.31	3.02
	SCI	1.60	2.01	2.55

V. Future work

1. Excitonic effect and scissors correction

(1) Large excitonic effects in linear optical spectra from monolayers

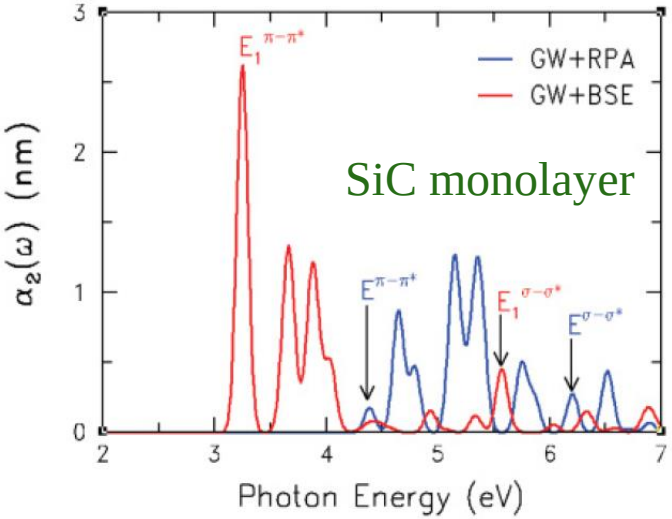

[Hsueh, Guo, Louie, PRB 84 (2011) 085404]

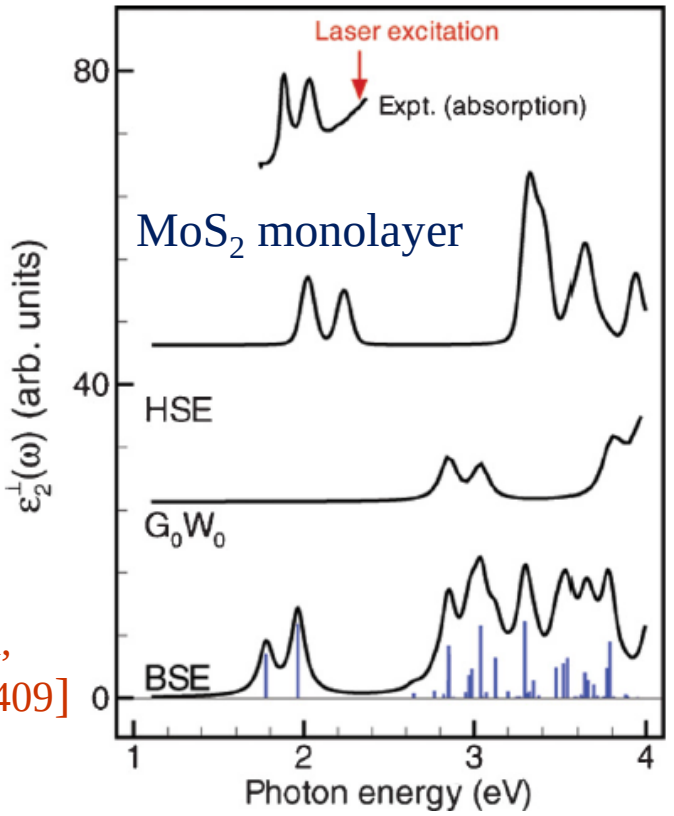

[Ramasubramaniam, PRB 86 (2012) 115409]

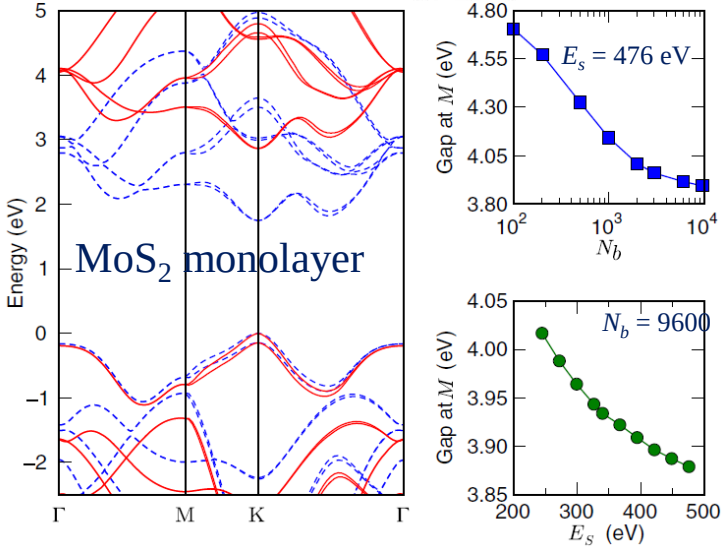

[Qiu, da Jornada, Louie, PRL 111 (2013) 216805]

Converged calculations are challenging.

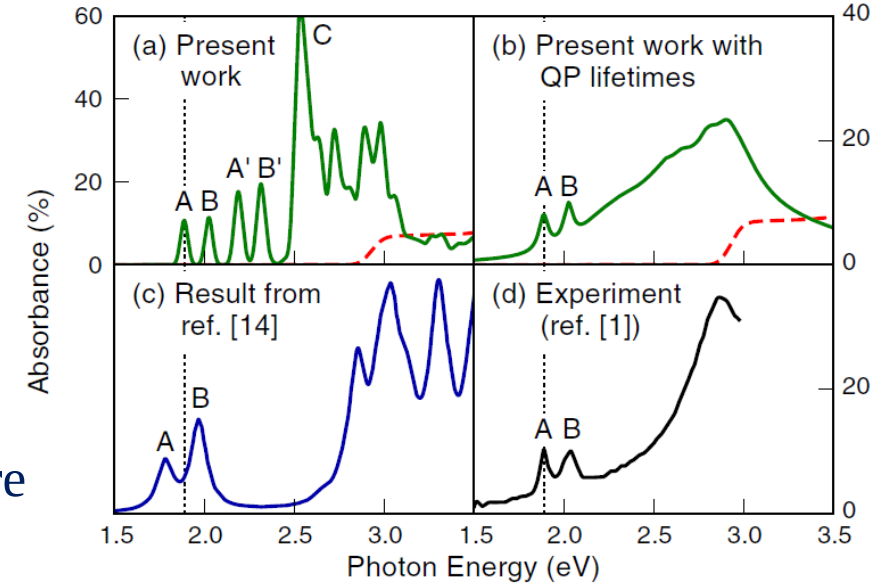

(2) Calculation of second-harmonic generation including the electron-hole interaction

State-of-the-art ab initio calculation of SHG with the GW-BSE formalism is extremely complicated and unpractically demanding.

[Gruning, Attaccalite PRB 89 (2014) 081102]

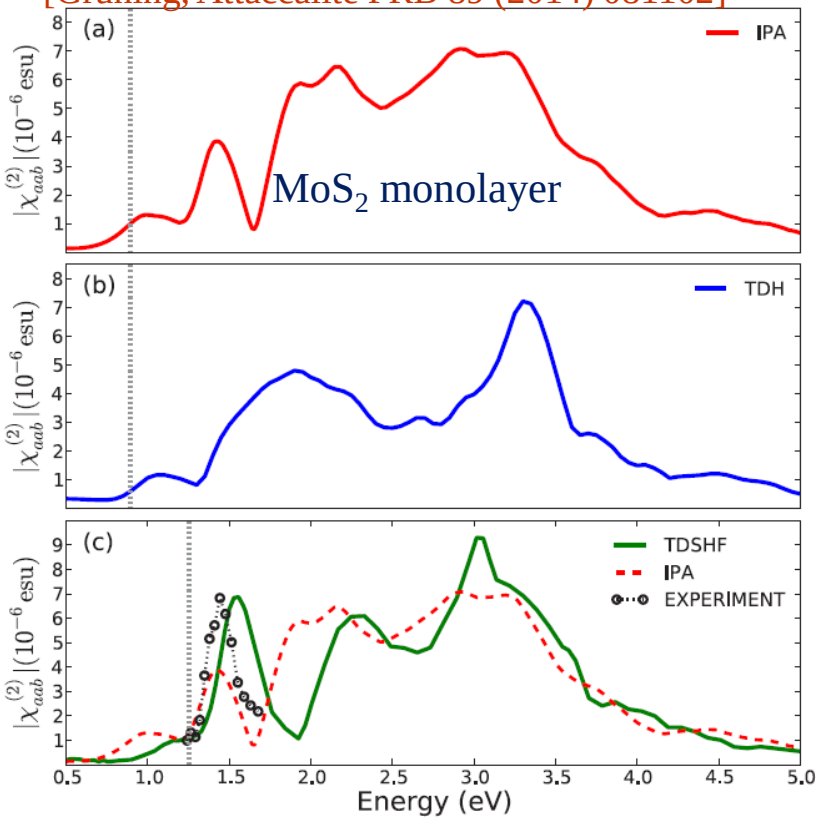

A real-time ab initio approach: Many-body effects are included as an operator into time-dependent Hamiltonian.

[Trolle et al., PRB 89 (2014) 235410]

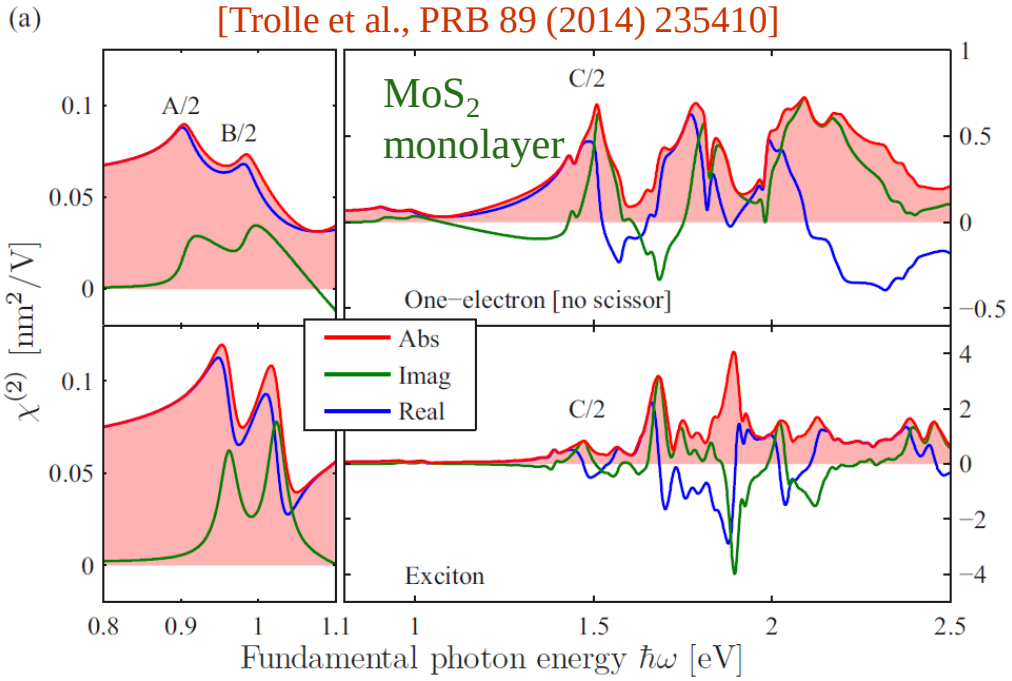

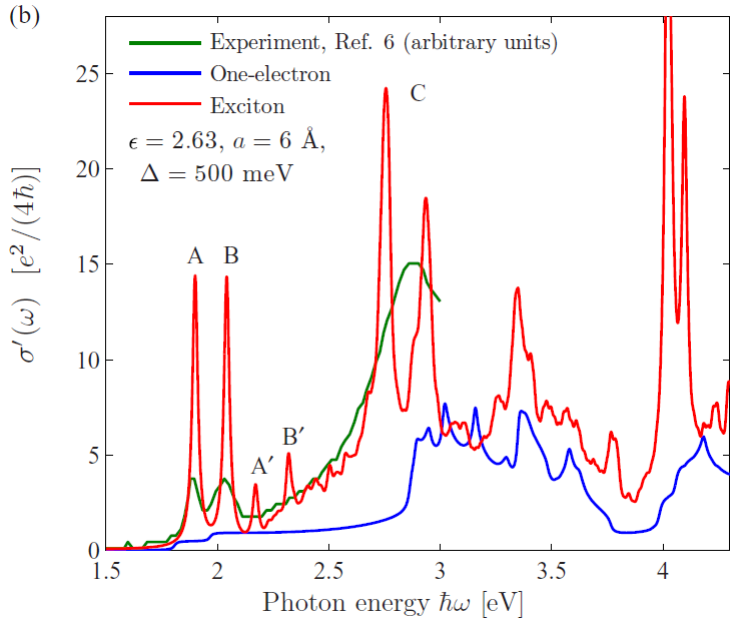

A semiempirical tight-binding approach.

(3) Independent particle approximation plus scissors correction

Unlike linear optical properties, the excitonic effects appear to be washed out to some extent. Thus, the IPA+scissors correction approach seems to be capable of producing reasonable results. On the other hand, this simpler approach allows one to use a sufficiently dense k-mesh and to include sufficiently large number of empty bands, which are crucial to get numerically converged SHG.

[Wang, Guo, JPCC 119 (2015) 13268]

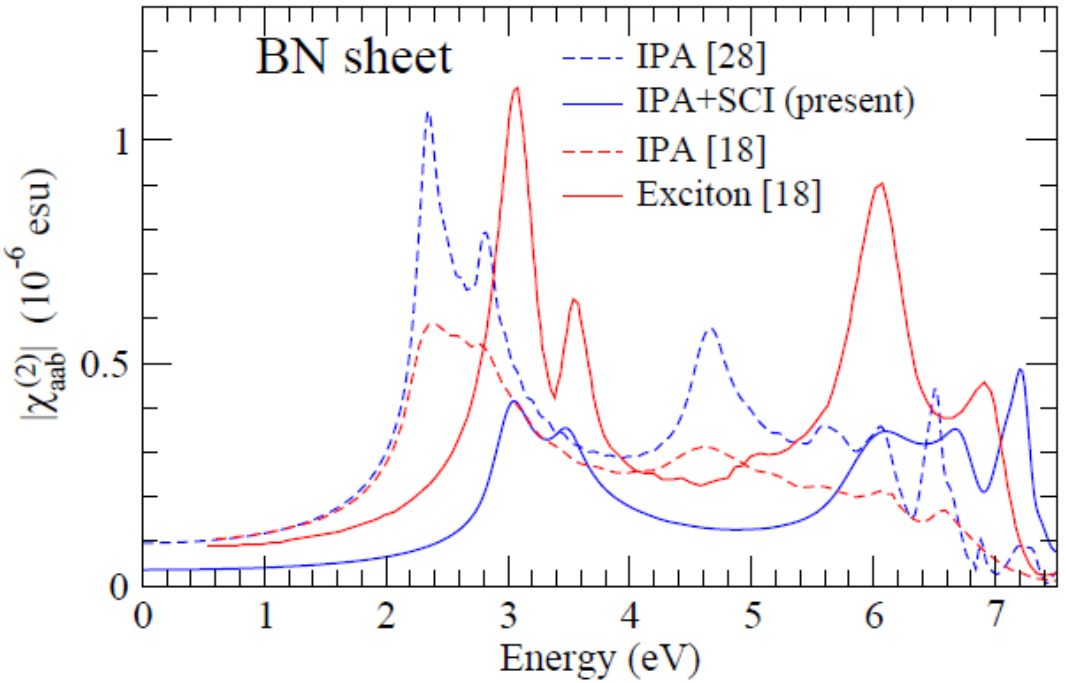

[18] Gruning, Attaccalite, PRB 89 (2014) 081102.
[28] Guo, Lin, PRB 72 (2005) 075416.

2. Time-propagation approach

Plan: To collaborate with Prof. Gross' group to develop a real-time ab initio approach where many-body effects are included as an operator into time-dependent Hamiltonian and implement it in the ELK.

[Gruning, Attaccalite PRB 89 (2014) 081102]